Journal of Hydraulic Structures
J. Hydraul. Struct., 2023; 9(2): 48-74
DOI: 10.22055/jhs.2023.44288.1259

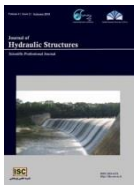

OPEN ACCESS

Uncertainty Quantification of Steady-State Seepage Through Earth-fill Dams by Random Finite Element Method and Multivariate Adaptive Regression Splines

Milad Kheiry[1]
Farhoud Kalateh[2]

Abstract

This paper aims to investigate the effects of uncertainty in soil characteristics and dam geometry on seepage flow using the hybrid Multivariate Adaptive Regression Splines (MARS) and Monte Carlo Method (MCM). A computer program based on Darcy flow is developed in the Fortran language to calculate the discharge flow. After validating the numerical FORTRAN code with experimental outputs, firstly, the Deterministic Finite Element Method (DFEM) was used to obtain Seepage Exit Discharge (SED) in Steady State Condition (SSC), and MCM was used for probabilistic analysis to account for uncertainty in random parameters. The program monitored Pore Water Pressure (PWP) changes and integrated them into the time/space domains. To ensure minimal error, the results of the models were compared by Standard Error Calculation (SEC). The research also introduced a new component to compare the seepage flow resulting from the analysis of models in a dimensionless manner called the Effective Discharge MARSplines (EDM). In the present research, the combination of Machine Learning (ML) and MCM algorithms was used in an innovative way for Random Finite Element Method (RFEM) calculations. The results of the research indicate that a 17.9% increase in the H_d/H_u ratio in the deterministic analysis results in a 29.3% decrease in EDM, while in the probabilistic analysis, a similar increase leads to a 19.02% decrease in EDM. Upon comparing deterministic and stochastic models, it can be concluded that deterministic analysis is more accurate and exhibits less error when compared to the probabilistic model.

Keywords: FORTRAN Programming; Seepage Exit Discharge (SED); Two-Phase Soil; Stochastic Analysis; Computational Fluid Dynamics.

Received: 14 July 2023; Accepted: 04 August 2023

1. Introduction

Seepage Analysis (SA) is one of the most essential problems in earth/rockfill dam engineering as it reveals potential water paths through porous media and evaluate the risk of piping, internal erosion, and stability failures. Over the past century, seepage through earth and rockfill dams has emerged as a significant and widespread cause of failure. [1-4]. The MARS method is a data-

[1] Faculty of Civil Engineering, University of Tabriz, East Azerbaijan Province, Tabriz, Iran.
[2] Faculty of Civil Engineering, University of Tabriz, East Azerbaijan Province, Tabriz, Iran. E-Mail: Fkalateh@tabrizu.ac.ir, Tel: +989144154062 **(Corresponding author)**

driven technique applied in various fields, especially geo-technical and geo-mechanical issues, and is computationally efficient method that builds flexible models using splines context and approximates the model using a set of basic functions. Zhang & Goh [5] used MARS for geotechnical systems and compared it with other machine learning methods. Their result indicated that MARS outperformed other methods regarding accuracy and computational efficiency, and also showed that MARS effectively analyzed relationships between permeability, rock quality designation, and depth of soil/rock. MARS has been used in various studies related to geotechnical engineering, including slope stability analysis 2D/3D slope stability analysis in anisotropic and heterogeneous soils [6], reliability analysis of slope failure [7], and permeability correlation between [8].

Several studies have demonstrated the effectiveness of MARS in dam problems, for example, in a study by Kumar *et al* [9], MARS was used to perform a reliability analysis of the slope failure of the Durgawati earth dam that located in India. The study calculated the β reliability index using MARS method under steady and unsteady seepage conditions. The Factor of Safety (FOS) of the Durgawati dam was computed using a modified Bishop's method, and seepage and slope stability analysis were performed using Geo Studio (2007) software include; SEEP/W and SLOPE-W subprograms.

Wang *et al* [10] introduced a high-performance stochastic stability investigation method for earth dams using MARS and soft computing algorithm. This approach is applied for the Ashigong earth dam under transient seepage, and the study systematically explores the effects of uncertainties of soil parameters and water level fluctuation on the slope failure of probability. Zheng *et al* [11] presented an approach for estimating the liquefaction-induced settlement of buildings with shallow foundations. Their method utilizes the MARS algorithm and artificial intelligence (AI) that its data is generated through the various finite difference method (FDM) analysis. The AI data cover various properties of the soil, structure, and ground motion. The impact of each input parameter and their coupled interactions on the liquefaction-induced settlement is quantified using several relative analyses executed using MARS.

Vu *et al* [12] suggests a new data-driven method for predicting potential of soil erosion using MARS and the Social Spider Algorithm (SSA). By fine-tuning hyper-parameters, SSA optimizes MARS performance by separating input data into 'erosion' and 'non-erosion' regions. The method proposed by Deng *et al* [13] combines sliced inverse regression (SIR) and MARS to effectively establish the relationship between soil properties and safety factors. In their work, Karhunen-Loeve expansion (K-L) is used to simulate soil variability, and the method is validated with one- or two-layer slopes.

Aleatory uncertainty is related to randomness in nature, which considers the essence of nature and is known by the titles of external uncertainty, inherent uncertainty, objective uncertainty, random uncertainty, fundamental uncertainty, and real-world uncertainty. On the other hand, Epistemic uncertainty researches the state of human knowledge and information about a physical system and the ability to measure uncertainty. This type of uncertainty is known as functional, internal, subjective, and incompleteness [14].

Soil analysis is an important aspect of environmental science, and it involves dealing with different types of uncertainties. Aleatory uncertainty in soil analysis refers to the inherent randomness in nature, derived from natural variability of the physical world, such as the variability in soil properties due to different soil types, weather conditions, and other natural factors. Epistemic uncertainty, on the other hand, refers to the imperfection of knowledge, such as incomplete data, inadequate understanding of the underlying processes, or imprecise evaluation of the related characteristics. In soil analysis, epistemic uncertainty can arise from the lack of

information about the soil properties, such as the soil texture, organic matter content, and nutrient availability, which can affect the accuracy of the analysis results. Understanding and quantifying these uncertainties are crucial for the interpretation and communication of the soil analysis results and for making informed decisions based on the available information.

Zhang *et al* [15] proposed the Mesh-less Moving Kriging method (MMKM) with Monte Carlo Integration to address the seepage problem in a heterogeneous earth dam. This method eliminates the need for meshing in the creation of shape functions and numerical integration.

Ahmed *et al* [16] stated that the generation of the electric field is one of the effects of the flow of the seepage flow through the porous medium, which can be used to estimate the path and speed flow. Their plan was to use the Self-Potential Method (SPM) based on the electrical concept called Flow Potential Field (FPF) to remotely measure groundwater flow and also determine the path and velocity flow in the Earth dam with considering uncertainty and using Monte Carlo Markov Chains (MCMC). Fukumoto *et al* [17] solved the seepage flow estimation and boiling of saturated sandy soil due to seepage by Boltzmann network coupling and Discrete Element Method (DEM) in two-dimensional geometry.

Su *et al* [18] conducted an assessment of the seepage control mechanism under a dam using deterministic and uncertain approaches. They computed the seepage field and uncertain seepage field before and after implementing anti-seepage tools. Johari and Talebi [19] performed a stochastic analysis in unsaturated conditions, considering rainfall. They used the RFEM for uncertainty analysis of soil parameters. They developed a MATLAB program and utilized the soil-water retention curve (SWRC) to analyze slope instability alongside seepage flow. They also referenced a model proposed by Johari and Hooshmand-Nejad [20] to estimate the hysteretic SWRC in soil.

Zhao *et al* [21] conducted a three-dimensional study on embankment seepage using a combination of the Monte Carlo method and a three-dimensional multimedia random field. They varied the coefficient of variation (COV) and fluctuation scales to analyze seepage. The foundation was modeled in layers, and the multimedia random field was based on the local average subdivision technique.

By using 1000 cases soil samples for database, Johari, Heydari & Talebi [22] developed the Scaled Boundary Finite Element Method (SBFEM) for SA in the foundation of dam. Then, by MARS, an equation was created to predict seepage flow; input parameters for the MARS-based model include structure height, upstream water level, and anisotropy ratio of hydraulic conductivity.

Kalateh and Kheiry [23] conducted SA of homogeneous earth dams, focusing on the application of MCS. They investigated SED in different geometries of dams and slopes, and their findings revealed that the average SED computed with MCS analysis was lower than the SED values in deterministic model. This study highlights the significance of considering stochastic analysis and spatial variability in hydraulic parameters when assessing seepage in earth dams.

There are two main objectives of this research, include: a. Estimating the effect of uncertainty of soil hydraulic conductivity (SHC) in the SED of the dam b. Comparison deterministic and stochastic MARS methods for the calculation of the EDM considering Geometry, Soil properties as random variables. In general, an overview of process of this research is shown Figure 1.

In previous researches, RFEM was used to calculate seepage based on traditional algorithms that, in this research, by using a new method based on the combination of two algorithms of ML and MCM, SED analysis is calculated probabilistically. Also, in the current research, a new parameter called EDM was used to compare the results, which provides the possibility of dimensionless comparison.

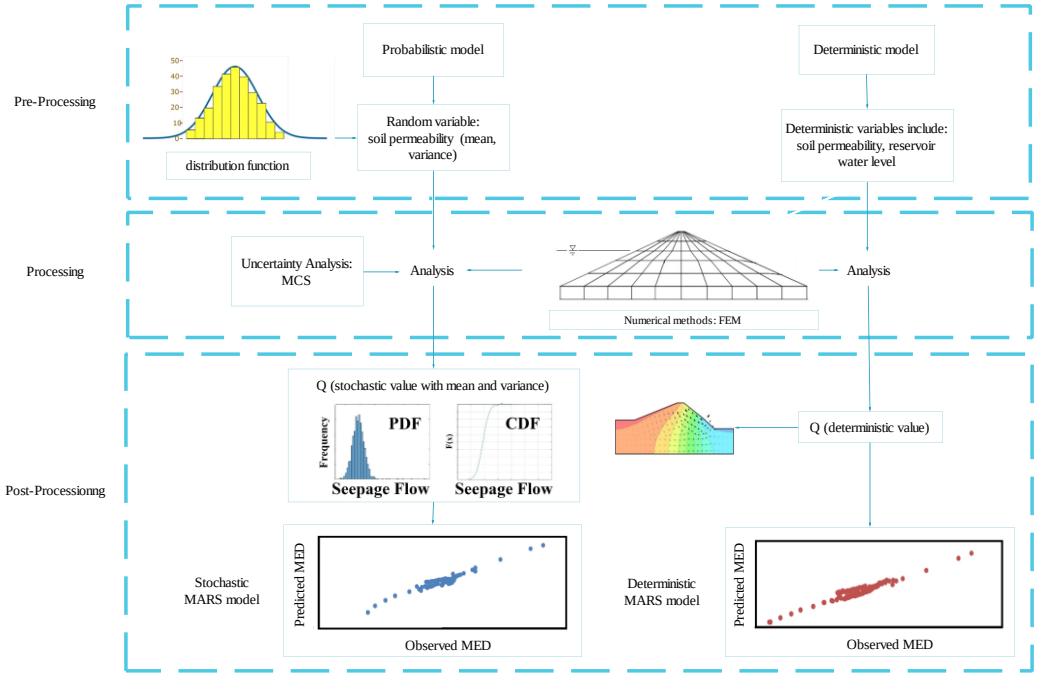

Figure 1. An overview of the comparison of two deterministic and probabilistic methods in the current study.

2. METHODS

To numerically solve the Hydro-Mechanical equations in the porous medium, Smith & Griffiths [24] have written a code in the FORTRAN programming language that calculates the Seepage flow rate and hydraulic head in the homogeneous and heterogeneous earth dams. This code is written in a deterministic manner, which in this research has been tried to be developed by considering uncertainty and converting MCS. In this research, the uncertainty of the dam has been analyzed with the hybrid algorithm of the MCS and MARS methods, which is shown schematically in Figure 2.

This FORTRAN code for solving seepage equations is similar to solid mechanics of problem codes that are inspired by the solution of static and dynamic equilibrium calculations. By using the finite element method, Laplace's differential equation is solved; however, instead of displacement and force variables in mechanic problems, PWP and seepage discharge are used.

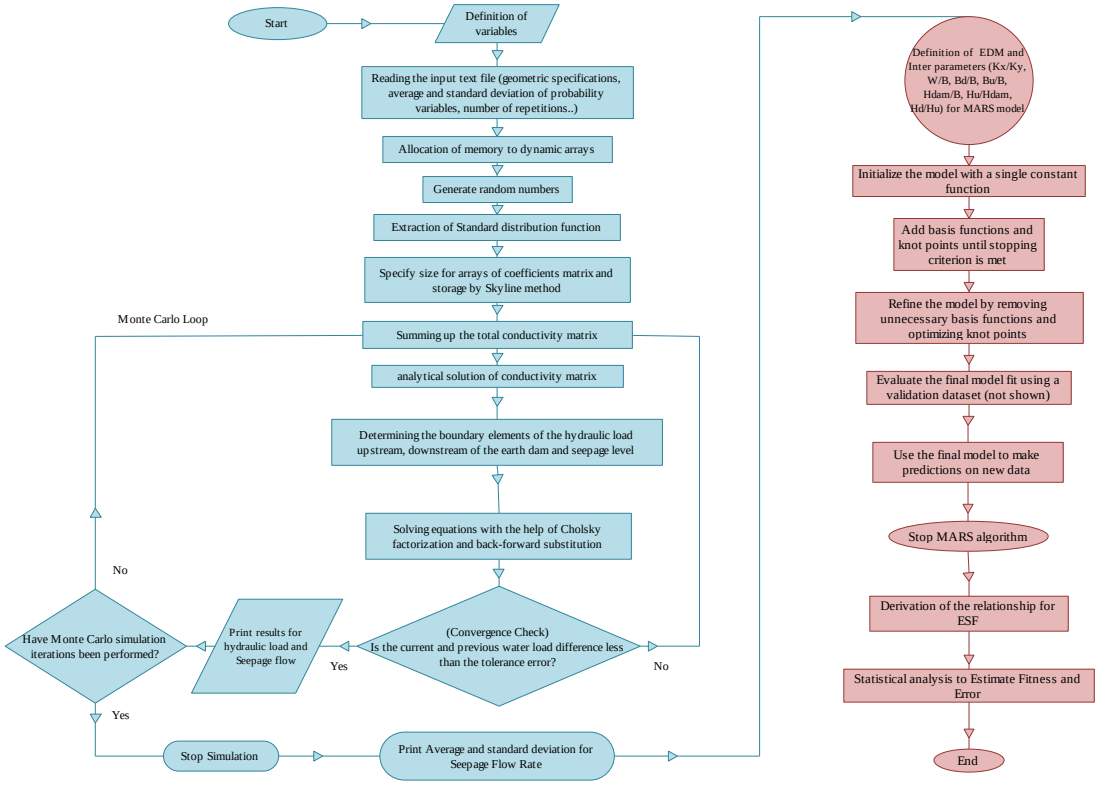

Figure 2. Process of MCS- MARS algorithm to use in the present research.

Governing equations

The Seepage flow in porous structures is a challenging phenomenon that can be analyzed using the Laplace or Poisson equation. While Poisson's equation is commonly used as the governing equation for seepage flow, Laplace's equation provides a more comprehensive understanding of the underlying physics. The general form of Laplace's equation is:

$$k_x \frac{\partial^2 \varphi}{\partial x^2} + k_y \frac{\partial^2 \varphi}{\partial y^2} = q \tag{1}$$

In equation (1), K_y and K_x are the soil permeability(m/s) in vertical and horizontal axes respectively, φ means fluid flow potential or piezometer head (m), which q represents the SED which its unit is m^3/s. Equation (1) applies to steady flow in a homogeneous soil medium. However, in unsteady conditions, the equation must be modified to account for changes in hydraulic head over time:

$$\frac{\partial}{\partial x}(k_x \frac{\partial p}{\partial x}) + \frac{\partial}{\partial y}(k_y \frac{\partial p}{\partial y}) = q + \frac{\partial \theta}{\partial t} \tag{2}$$

In equation (2), p is hydraulic head (m) and ∂θ/∂t is the humidity volume changes into porous media with time. The Laplace formula for steady state can also be represent:

$$k_x \frac{\partial^2 \varphi}{\partial x^2} + k_y \frac{\partial^2 \varphi}{\partial y^2} = 0 \quad (3)$$

Through the utilization of the FEM and discretization of the equation (3), it is transformed into following equation:

$$[k_c]\{\varphi\} = \{q\} \quad (4)$$

In equation (4), global symmetric coefficients matrix is $[K_c]$, the vector nodal of hydraulic head $\{\varphi\}$, and the SED vector$\{q\}$. Using the FEM, equation (4) is changed:

$$\varphi = [N]\{\varphi\} \quad (5)$$

The weight function and the shape function are the same (W_i=N_i), so the general form of the *[Kc]* matrix is written as follows:

$$\iint \left(k_x \frac{\partial N_i}{\partial x}\frac{\partial N_i}{\partial x} + k_y \frac{\partial N_i}{\partial y}\frac{\partial N_i}{\partial y}\right) dxdy = 0 \quad (6)$$

Furthermore, it is possible to express the matrix of coefficients in the following manner:

$$[K_c] = \iint ([T]^T [K][T])\, dxdy \quad (7)$$

The matrix of properties [K] is:

$$K = \begin{bmatrix} k_x & 0 \\ 0 & k_y \end{bmatrix} \quad (8)$$

If we make the assumption that the primary axes of the permeability tensor align with the x and y coordinate axis, then the matrix [T] bears a resemblance to the matrix [B] commonly encountered in concept mechanics of solid.

MARS computational method

In recent years, the use of ML and soft computing methods has caused a revolution in the modeling of hydraulic structures, and many researchers have used these methods to predict the behavior of hydraulic structures [25-29]. Analysis of steady and unsteady water flow has been one of the basic applications of soft computing [29-32]. MARS algorithm, which was first introduced by Friedman [33], has become a well-liked non-parametric regression technique due to its high flexibility and accuracy [34]. The MARS method can be used for both regression and classification problems. For regression problems, the MARS model predicts the value of a continuous response

variable, while for classification problems, the MARS model predicts the probability of a binary or multi-class response variable.

The MARS method is a deep non-parametric data driven technique that can be used to model complex relationships between a response variable and multiple predictor variables. The MARS model is constructed by combining basis functions in a linear and nonlinear way, and it can be used for both regression and classification problems. The MARS method is particularly useful for processing high-dimensional data and large data samples (Figure 3).

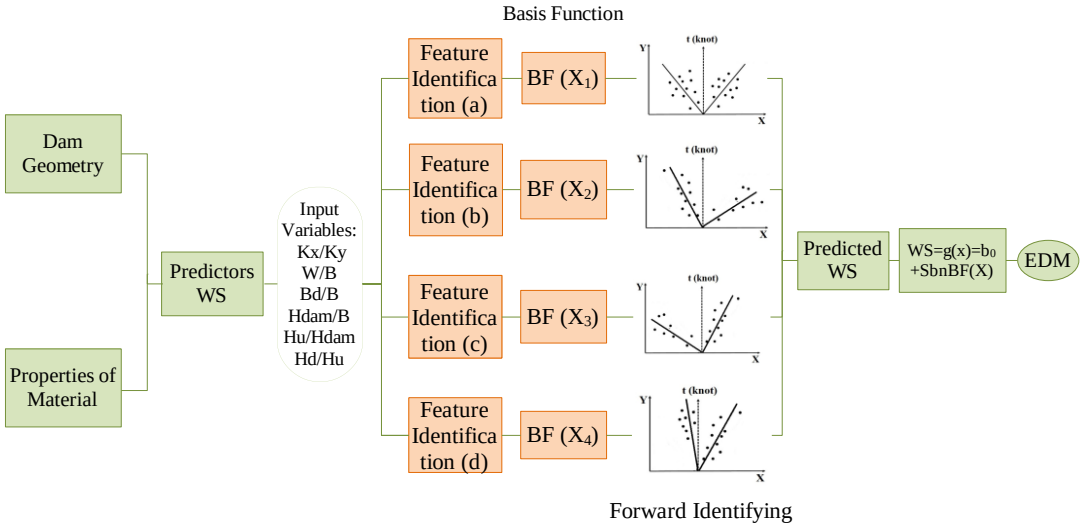

Figure 3. Using MARS algorithm from basis function for predicting.

The advantage of MARS is to model complex relationships between a response variable and multiple predictor variables. The MARS method is a combination of Recursive Partitioning Regression (RPR) and the Spline method, which allows for the processing of high-dimensional data (data that has many predictor variables) and large data samples. The MARS model is obtained by a combination of Basis Function values (BF), Maximum Interaction (MI), and Minimum Observation (MO) by trial and error. The Basis Function values are the building blocks of the MARS model, and they are used to construct the model by combining them in a linear or nonlinear way.

MARS can handle missing data by using a technique called "backfitting." Here is how it works: a) The model is first fit to the complete cases, which are the cases with no missing data. b) The model is then used to impute the missing values for each incomplete case. c) This is done by predicting the missing value using the model and the available values for that case. d) The imputed values are then used to update the model. e) This is done by refitting the model to the complete cases and the imputed values for the incomplete cases. f) The process of imputing missing values and updating the model is repeated until convergence is achieved.

Backfitting is an iterative algorithm that can handle missing data in a flexible and efficient way. It allows MARS to use all available data to estimate the model parameters, even when some data is missing. However, it is important to note that the accuracy of the imputed values depends on the quality of the model and the available data. Therefore, it is important to carefully evaluate the imputed values and the overall performance of the model when dealing with missing data.

The MARS builds a model by partitioning the input space into smaller regions and fitting a linear regression model to each region. The basis equation governing the MARS algorithm can be written as follows:

$$y = \beta_0 + \sum j = 1 \; to \; M. \beta_j . B_j(x) \tag{9}$$

where y is the response variable, x is the vector of predictor variables, β_0 is the intercept term, βj are the coefficients for the basic functions $B_j(x)$, and M is the total number of basic functions used in the model. The basic functions used in MARS are piecewise linear functions called "hinge functions" and "constant functions". The hinge functions are defined as:

$$B_j(x) = \max(0, x - t) \quad for \quad x \geq t \tag{10}$$
$$B_j(x) = 0 \quad for \quad x < t \tag{11}$$

where t is the knot point that determines the location of the hinge function. The constant functions are defined as:

$$B_j(x) \; = \; 1 \, for \; all \; x \tag{12}$$

The MARS algorithm uses a forward stepwise approach to select the best set of basic functions and knot points that minimize the sum of squared residuals between the predicted values and the actual values. The algorithm starts with a single constant function and adds hinge functions one at a time until a stopping criterion is met. The stopping criterion can be based on a maximum number of basic functions, a minimum improvement in the model fit, or a maximum complexity penalty. Overall, the MARS algorithm is a flexible and powerful method for modeling complex relationships between multiple predictor variables and a response variable.

The weight of the smoothness penalty (WS) is a hyperparameter that controls the strength of the penalty term. A higher value of WS results in a smoother model with fewer knots, while a lower value of WS allows for more flexibility and more knots in the model. The optimal value of WS depends on the complexity of the data and the trade-off between bias and variance in the model. WS is a hyperparameter in MARS that controls the smoothness of the model and helps to prevent overfitting.

MSC formulation

Given a PDF for a stochastic variable X, the set of values for which (x) is positive is determined. The expected value of X can then be calculated, resulting in a solution expressed as a function g(X).

$$\mathbb{E}\big(g(X)\big) = \sum_{x \epsilon X} g(x) f_X(x) \tag{13}$$

So, if X is discrete, and

$$\mathbb{E}\big(g(X)\big) = \int_{x \epsilon X} g(x) fX(x) dx \tag{14}$$

To compute the average g(x) for total samples can considered MSC method as:

$$\widetilde{g_n}(x) = \frac{1}{n}\sum_{i=1}^{n} g(x_i) \tag{15}$$

Which we call the Monte Carlo estimator of *E(g(X))*. If *E(g(X))*, exists, at that point the weak law of high numbers tells us that for any arbitrary little ε:

$$\lim_{n\to\infty} P\left(\left|\widetilde{g_n}(X) - \mathbb{E}\left(g(X)\right)\right| \geq \epsilon\right) = 0 \tag{16}$$

In the FORTRAN code of this study, iteration loops are used for MCM, and according to Figure 2, in order to check the convergence, a sub-program has been created for all elements continuously in a loop that compares the hydraulic head difference obtained in the n iteration with its achieved value in the n-1 iteration, and if this difference is less than the tolerance error, then the program stops. In the next part of the algorithm, the data obtained from the repeated executions of the FORTRAN program inter in the MARS model is a connection between the EDM and input variables.

Statistical Indexes

In the second step, next to the modeling of the FORTRAN program, the data is analyzed by the MARS method. The result of these two processes is presented in the form of a specific equation for two deterministic and probabilistic conditions, and at this step, the error values of the equations should be investigated by statistical measures. The Statistical indices include; Coefficient of Determination (R^2), Root Mean Square Error (*RMSE*), Mean Absolute Error (*MAE*), Relative Root Mean Square Error (*RRMSE*), and Relative Standard Error (*RSE*) were used, which are defined as follows [35, 36]:

$$MAE = \frac{\sum_{i=1}^{n}|fm_i - gm_i|}{n}, \tag{17}$$

$$RSE = \frac{\sum_{i=1}^{n}(gm_i - fm_i)^2}{\sum_{i=1}^{n}(\overline{fm} - fm_i)^2}, \tag{18}$$

$$RRMSE = \frac{1}{e}\sqrt{\frac{\sum_{i=1}^{n}(fm_i - gm_i)^2}{n}} \tag{19}$$

$$R = \frac{\sum_{i=1}^{n}(fm_i - \overline{fm})(gm_i - \overline{gm_i})}{\sqrt{\sum_{i=1}^{n}(fm_i - \overline{fm})^2 \sum_{i=1}^{n}(gm_i - \overline{gm_i})^2}}, \tag{20}$$

$$\rho = \frac{RRMSE}{1+R}, \tag{21}$$

Validation of computational program

Numerical models need to be compared with laboratory or field models to ensure the validity of the results. In the present research, the experimental model of Kouhpeyma *et al* [37] was used for validation, which was implemented in a Flume with dimensions of 1.1, 1, and 0.15 m for the length, height, and width of the tank, respectively. The dimensions of physical modeling (Figure 4) were chosen on a small scale, but granular soil was selected based on real materials. For seepage modeling, a water tank was used, which is equipped with 11 piezometers at horizontal distances

of 10 cm from each other on the base and two pipe overflows in the downstream and upstream tanks to adjust the water level (Figure 5).

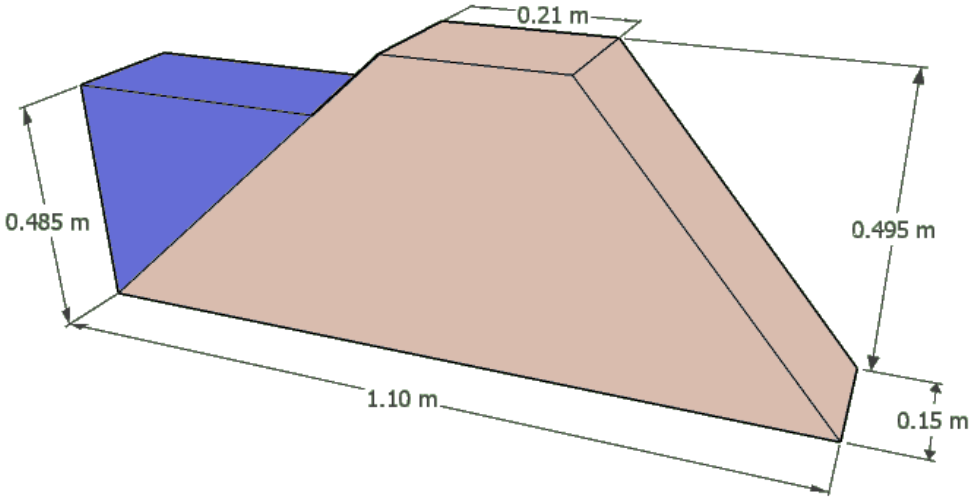

Figure 4. The 3D geometry of the physical model of the earth dam by [37].

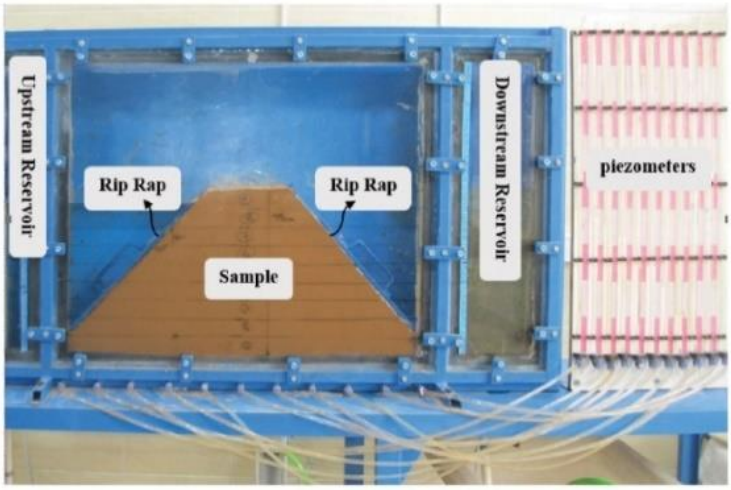

Figure 5. View of the physical model of Kouhpeyma *et al* [37].

The amount of seepage for reservoir level equal to 0.495 m of the reservoir and for the dam body with the properties of the Figure 4 was calculated by the numerical model, and the results of the seepage and hydraulic head were compared with the experimental outputs (Figure 6). Also, according to Table 1, the difference between the numerical values obtained from the FORTRAN program and the laboratory data dam is very low and about 0.31%.

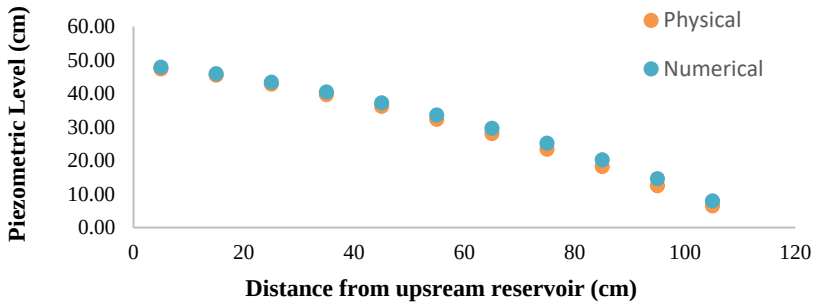

Figure 6. Comparison of hydraulic head obtained from the physical model of Kouhpeyma *et al* [37] with the numerical results of the present study.

Table 1. Comparison of Seepage rate results in Earth dam with laboratory model.

Parameter	Seepage Discharge (Numerical model of the present Study) $\times 10^{-7}$ m3/s	Seepage Flow (Experimental model) $\times 10^{-7}$ m3/s	Differences between Experimental and Numerical) $\times 10^{-7}$ m3/s	Percentage Error %
Quantity	4.83	4.85	0.02	0.31

Mesh Convergency Check

Upon achieving convergence, additional mesh refinement no longer affects the results, and the model and its outcomes become independent of the mesh. This mesh convergence study serves to verify that the FEA model converges to a solution and to justify the mesh independence. The study involves altering the size and configuration of the FEA mesh by disabling the automatic meshing feature of the FEA solver and modifying the mesh parameters in three directions. The number of elements along each edge is incrementally increased, and the complexity of the model is recorded against the response. The response of interest is the maximum vertical deflection, and the solution time is also recorded. A data of mesh size versus deviation and solution time is generated, and the maximum vertical deviation is plotted against the number of elements in the model. At some point, the system response converges to a solution.

In the case of the mesh convergence test at hand, six different mesh sizes were utilized, with the number of elements ranging from 9 to 1000. The largest mesh had only 9 elements, while the smallest had 1000 elements (Figure 7). The other mesh sizes used were 25, 50, 70, and 450 elements as presented in Table 2. Through a comparison of the results obtained from each mesh size, the optimal mesh size for the simulation can be determined. In the "Mesh Convergence Check" section, a sensitivity analysis is required to achieve the optimal mesh. If a very fine mesh is selected, the program execution time will be significantly long and time-consuming. On the other hand, if a much larger element is used, the results will deviate from reality. Therefore, to ensure the suitability of the meshing and the size of the elements, the mesh convergence analysis stage was performed, and its results are presented in the Table 2.

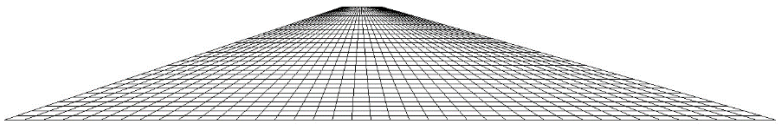

Figure 7. The smallest mesh size for finite element modelling with 1000 elements.

Table 2. The convergency test of types of meshing in finite element analysis.

No. of meshing	No.1	No.2	No.3	No.4	No.5	No.6	No.7
Number of all Nodes	40	96	181	245	1281	1911	3131
Number of Elements	9	25	50	70	200	450	1000
Time of solving (t/t1000)	0.05	0.16	0.22	0.31	0.52	0.69	1
EDM (Deterministic)	7.85	6.12	5.02	4.81	4.83	4.83	4.83
EDM (Stochastic)	10.22	8.75	6.75	5.25	5.17	5.16	5.16
Type Element	4-node quadrilateral element						

FEM-based Programming for seepage analysis

The input random variable for MCS is the conductivity coefficient of the soil along with the deterministic input variables, and the random output variable is seepage flow through the dam. The soil conductivity variable, as a stochastic variable, has a mean and a standard deviation (SD). MCS has been performed with 2000 iterations, and in contrast to the deterministic analysis, a number of iteration SED values have been obtained, which requires the use of a PDF to display these results. The paper is modeled in three phases: geometry, reservoir water and downstream water levels, and soil permeability. Each of the models has been implemented in the FORTRAN program, and finally, deterministic and probabilistic results were compared.

As discussed in Hydro-Mechanical problems, the free surface flow problem includes an upper boundary, and the position of this boundary is not known beforehand (the first flow line or percolation front), so an iterative process will be necessary to find such a boundary. In fact, the unknown position of one of the boundaries of the solution domain causes the problem to become nonlinear. For example, a fixed finite element mesh can be used, and the nodes can be divided into two regions of active and inactive nodes, depending on whether the fluid is present in that node or not. The other method is the method used in the present program, in such a way that the meshing of the finite elements takes place in time steps, and finally, the upper surface of the meshing coincides with the free surface of the flow.

In the deterministic model, the analysis starts with the assumption of a known initial position for the free surface, and the solution of the Laplace equation determines the values of the total water charge in the nodes located along the free surface of the flow, which in the general condition are not the same as the level of the upper surface of the mesh of finite elements. Therefore, the level of the nodes located in the boundary of the upper surface is compared with the values of the hydraulic head calculated in this step, and in other words, the nodal coordinates of the points located on the upper boundary of the free surface are corrected and with the total hydraulic head obtained by solving the equation Laplace is set equal. In order to avoid distorted elements, the Geom_Freesurf subroutine is used, ensuring that the nodes beneath the top surface are evenly distributed. This geometric subroutine is created to help to solve the seepage problem with a free

surface, an initial domain of trapezoidal meshing, and counting the nodes and elements along the x-axis. Then the analysis, solving the Laplace equation, is repeated for the new mesh.

Since the coordinates of many nodal points in the mesh of finite elements change, the matrix of coefficients of all the elements must be recomputed and assembled into the global system. In order to avoid numerical integration in determining the values of the matrix coefficients of each element, an analytical-computational method is used by subroutine seep4. Library subroutine Seep4 calculated the conductivity matrices kc for the element "analytically". In general, the assembly is made into a global conductivity matrix k_v stored as a skyline.

In this program, the subroutine for generating the mesh and nodal coordinates of the domain has not been solved, therefore, in the input file, the coordinates of each nodal point Coord_g and also the pattern of connecting the nodal points in each element Num_g should be introduced. In addition, some of the variables that previously had a fixed value in this program must be introduced as input variables in order to specify the geometry of the desired solution domain in the input file.

To solve problems of partial differential equations such as seepage and with the Deterministic Finite Element Method (DFEM), only average input data obtained from previous experimental results are considered, and the output variable is a single and unique data. In this output mode, it is not able to accurately explain the uncertainties caused by the random input variables [38, 39].

One of the main effective factors in the accuracy of the results in probabilistic methods based on the Monte Carlo method is the number of simulation iterations, which is selected based on the moving average of the results of the analyzes and for a certain level of acceptable error. In all analyzes of the present research, the number of iterations is 2000.

The main model for simulation is an earth dam with the geometry of Figure 8 and sand clay (SC) for the material. In the finite element mesh of the research, all the models have quadrilateral elements; for the upstream boundary, fixed nodal potential points equal to the height of the reservoir surface were used, and the downstream water level was considered proportional to the water height with fixed nodes. The boundary between the foundation and the dam is assumed to be zero discharge flow.

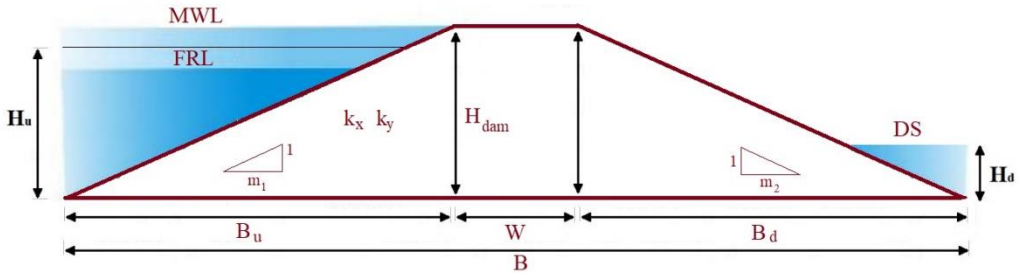

Figure 8. View of the Earth dam studying for boundary conditions in the present numerical model.

3. RESULTS AND DISCUSSION

Deterministic model

First, the program written in Fortran language is executed on the assumption that the permeability values of the materials are constant, and the results are expressed as two input and output leakage currents (in this case, these two values are equivalent). The result of the deterministic analysis shows that in the homogenous body where the vertical and horizontal

permeability is equal, the slope of the line is higher than in the two non-homogeneous models, and also, the effect of the horizontal component of permeability (Kx) is greater than its vertical component (Ky) on the discharge flow rate. In the deterministic model, two non-isotropic states are mentioned. In the first part, the value of the horizontal permeability component (Kx) is constant (3.33×10^{-7} m/s), and the vertical coefficient (Ky) is variable, and also in the second part, the value of the vertical permeability component is constant (3.33×10^{-7} m/s), and the horizontal penetration component is variable. With the increase of the downstream-to-upstream water level ratio (H_d/H_{up}), the amount of seepage has decreased. In fact, the seepage reduction is a linear function of the changing pattern (Hd/Hup), which is repeated for isotropic and non-isotropic conditions (Figure 9).

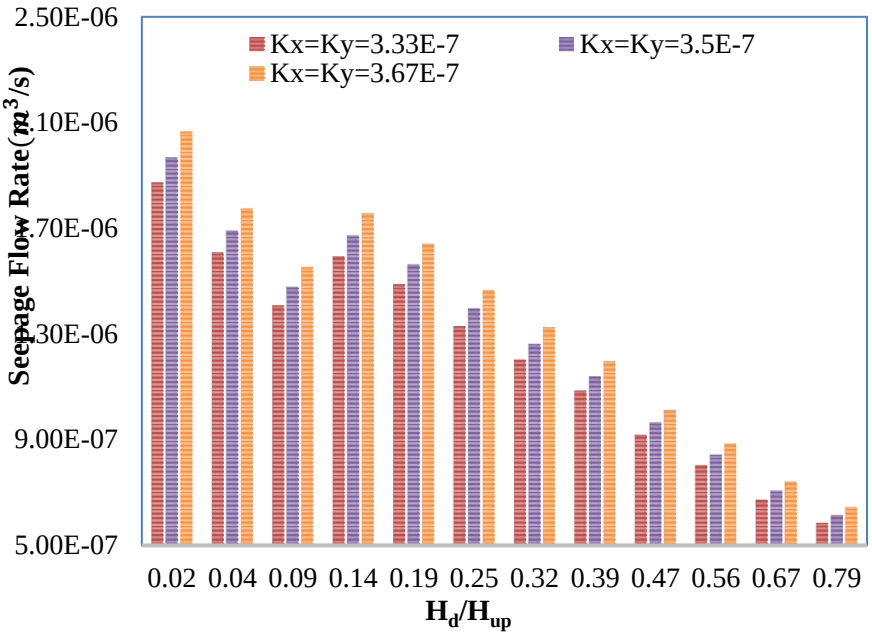

Figure 9. Relationship between ratio of downstream to upstream head (H_d/H_{up}) and SED in deterministic analysis.

Stochastic model

In the probabilistic model and the MCM, instead of the stability of hydraulic conductivity, its average and distribution functions are entered in the calculations. First, the dam was considered isotropic ($K_x=K_y$), and the code was executed in probabilistic mode. The resulting average discharge increases almost linearly with the increase of the hydraulic conductivity coefficient. Various Earth dams were modelled to investigate the scale effect on seepage, and then the models were entered into the probabilistic FORTRAN program. After that Probability distribution function (PDF) and Cumulative distribution function (CDF) graphs were extracted for each sub-model considering ratio of downstream water level to upstream (H_d/H_u) (Figure 10), the mentioned results in MARS were converted into equations for EDM calculation. In fact, Figure 10 presented PDF-CDF of diagrams for condition that H_d/H_u (height of downstream to upstream water level) is changing.

Hydraulic Conductivity of Soil

The related to Soil Hydraulic Conductivity (SHC) and in the specific mass of soil, the spatial heterogeneity of its layers is caused by the inherent variability of its structure and caused by processes such as sedimentation and natural soil weathering over passing years. In deterministic SA methods, a constant conservative value is considered for the properties of a single soil layer, and it is often assumed that the soil layers are homogeneous [40]. In contrast, probabilistic techniques assign wide values to material properties in each iteration instead of constant values.

If the values of the hydraulic conductivity coefficient of the dam body (K_x) are variable, the results of the running of the seepage code indicated the increase in the ratio of the horizontal conductivity to the vertical coefficient (K_x/K_y) soil. The average value of seepage in the range between 0.71 and 1 in the descending, again in the range of (1,1.41), is ascending. In fact, the linearity of the relationship between the mean seepage and K_x/K_y is not true. Note that according to Laplace equation, the assumption of nonlinearity of this relationship is close to reality. The SD has decreased with the increase in K_x/K_y ratio. The behaviors of maximum and minimum seepage rates are similar to the average flow in the probabilistic model for different values of K_x/K_y. In addition, the PDF and CDF have been compared in probabilistic models (Figure 11) and ranges of changing K_x/K_y is compared in Table 3.

Table 3. Changes in seepage behavior in probabilistic mode for changes K_x/K_y.

Horizontal to vertical permeability ratio Kx/Ky	Minimum of seepage flow $\times10^{-7}\times$m3/s	Maximum of seepage flow $\times10^{-7}\times$m3/	Average of seepage flow $\times10^{-7}\times$m3/s	standard deviation $\times10^{-7}$
0.71	6.146	19.19	11.54	1.768
0.75	6.082	18.91	11.5	1.747
0.78	6.024	18.65	11.46	1.727
0.82	5.969	18.39	11.42	1.709
0.86	5.918	18.15	11.38	1.693
0.91	5.87	17.91	11.34	1.678
0.95	5.826	17.69	11.3	1.664
1.00	5.784	17.46	11.27	1.651
1.05	6.308	17.96	11.79	1.644
1.10	6.888	18.47	12.34	1.637
1.16	7.498	19.01	12.92	1.63
1.22	8.134	19.57	13.52	1.622
1.28	8.796	20.17	14.15	1.614
1.34	9.49	20.79	14.82	1.607
1.41	10.21	21.44	15.51	1.601

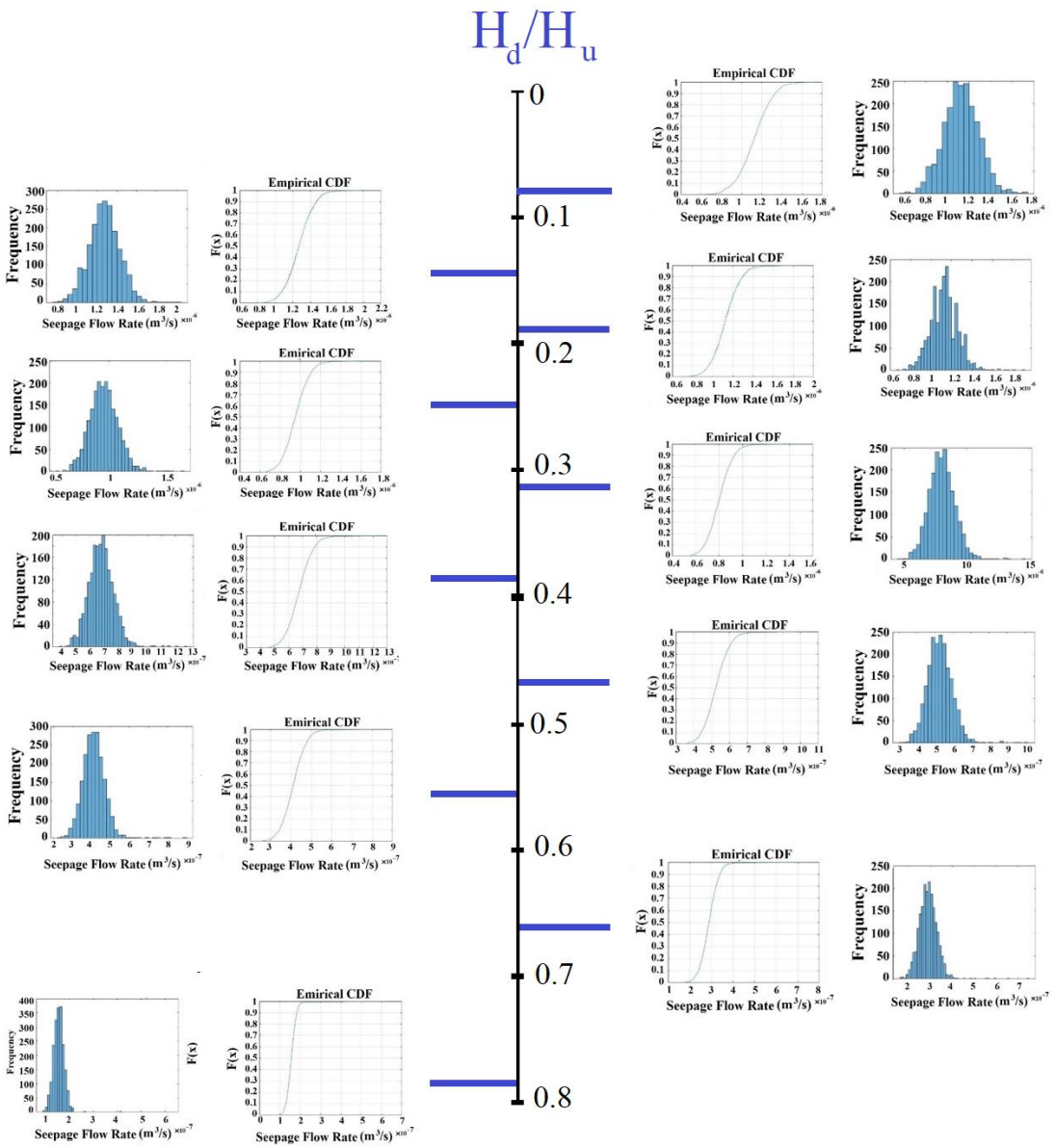

Figure 10. PDF and CDF diagrams for earth dam in change for reservoir and downstream water level changing (for Hd/Hu=0.09, 0.14, 0.19, 0.25, 0.32, 0.39, 0.47, 0.56, 0.67, and 0.79)

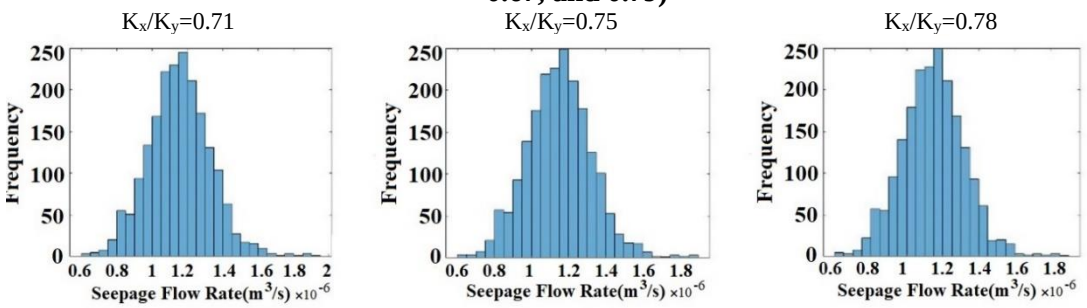

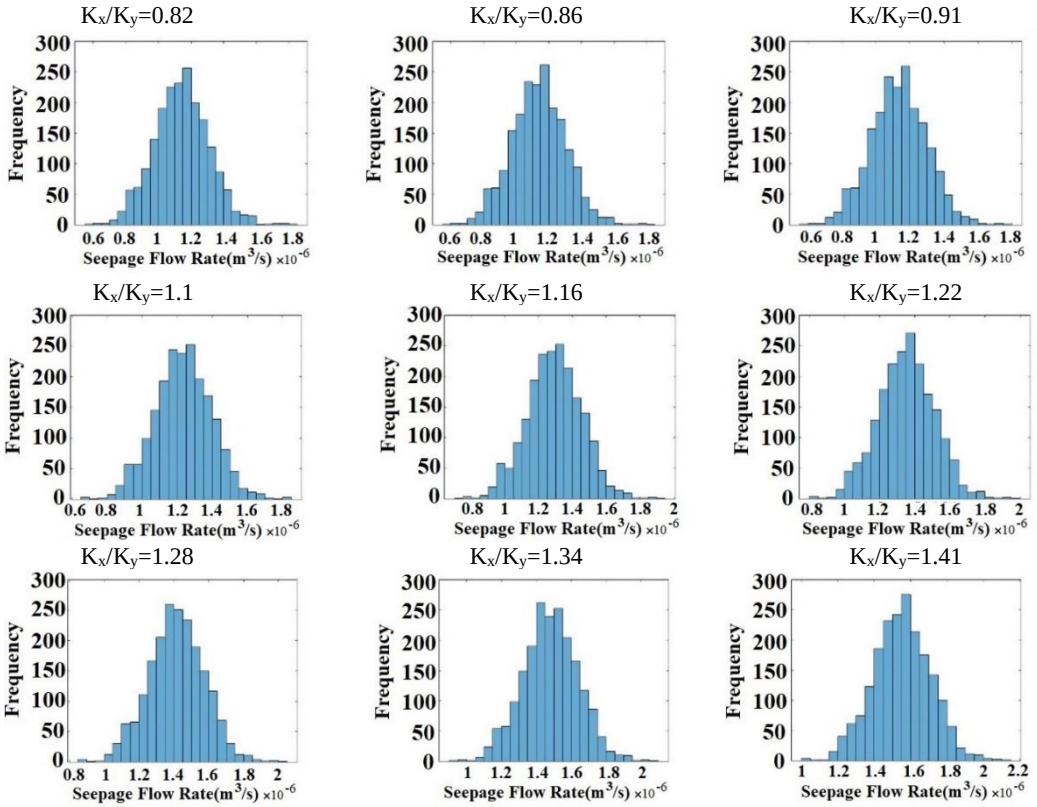

Figure 11. PDF including changes in horizontal to vertical conductivity ratio (K_x/K_y).

After several models of the Earth dam were run in the FORTRAN program, the mean and SD of the discharge rate in the deterministic and uncertainty models are obtained. With the aim of determining the relationship between the Effective Discharge of MARS method (EDM) rates (the Discharge variable is converted to the dimensionless variable called the EDM). $\frac{\text{Kx}}{\text{Ky}}$, $\frac{\text{W}}{\text{B}}$, $\frac{\text{Bd}}{\text{B}}$, $\frac{\text{Bu}}{\text{B}}$, $\frac{\text{Hdam}}{\text{B}}$, $\frac{\text{Hu}}{\text{Hdam}}$, and $\frac{\text{Hd}}{\text{Hu}}$ are input parameters that were used for the MARS model.

$$EDM = \frac{Q_{mean}}{K_{mean} \times H_{dam}} \tag{22}$$

In the above equation, EDM is the dimensionless discharge flow rate and Q_{mean} is the seepage flow rate from the body of the earthen dam in terms of cubic meters per second. Note that the variable is as average in probabilistic and deterministic analysis converted to Q which would be unique value (Not have a distribution function and SD). K is the average permeability coefficient body for two vertical axes Ky and horizontal Kx which are in m/s, and also H_{dam} is the dam height (m).

$$EDM = f\left(\frac{Kx}{Ky}, \frac{W}{B}, \frac{B_d}{B}, \frac{H_{dam}}{B}, \frac{H_u}{H_{dam}}, \frac{H_d}{H_u}\right) \tag{23}$$

Table 4 lists the descriptions of the input variables, that Figure 12 show minimum, maximum and medium of these parameters. Typically, the minimum crest width is not less than 3 m, even for small earth dams. In most large dams, this width is often between 6 and 12 m ranges and usually increases with the dam height incensement. The database resulting from the deterministic analysis is converted to continue analysis with the Data Driven algorithm.

Table 4. Statistical overview of the parameters for using MARS model.

Variable	Description
$\frac{Kx}{Ky}$	The ratio of horizontal to vertical soil permeability
$\frac{W}{B}$	The ratio of crest width to base width
$\frac{\mathrm{B_d}}{\mathrm{B}}$	The ratio of the crest distance from the downstream toe to base width
$\frac{H_d}{H}$	The ratio of the downstream water height to dam height
$\frac{H_u}{H}$	The ratio of the reservoir water height to dam height
$\frac{H_d}{H_u}$	The ratio of the downstream to upstream head

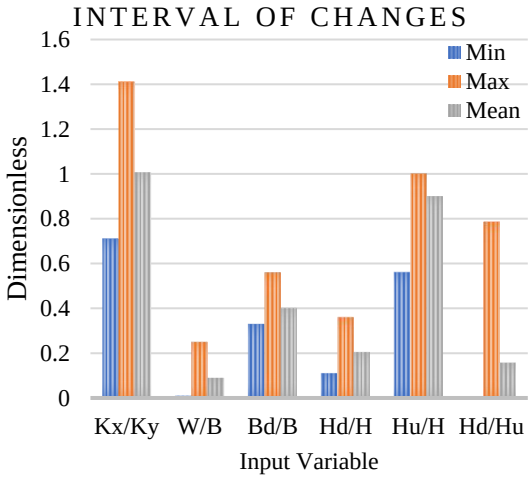

Figure 12. The range of changes of 6 input variables of the deterministic and stochastic models.

At first, The MARS model executes for deterministic data and starts by entering the input and output variables in the statistics software, and data is created for the model. In this case, MARS is a useful tool for earth dam analysis as it can capture the nonlinear relationships between various factors that affect the performance of an earth dam, especially SED analysis. Input variables included six items related to geometry, hydraulic conductivity coefficient, and water height upstream and downstream. Because the results can be generalized to other research, dimensionless variables were used for inputs and outputs. The results of the Mars method for comparing the values obtained from Mars and the data observed in the output of the uncertainty Fortran code are shown in Figure 13.

a

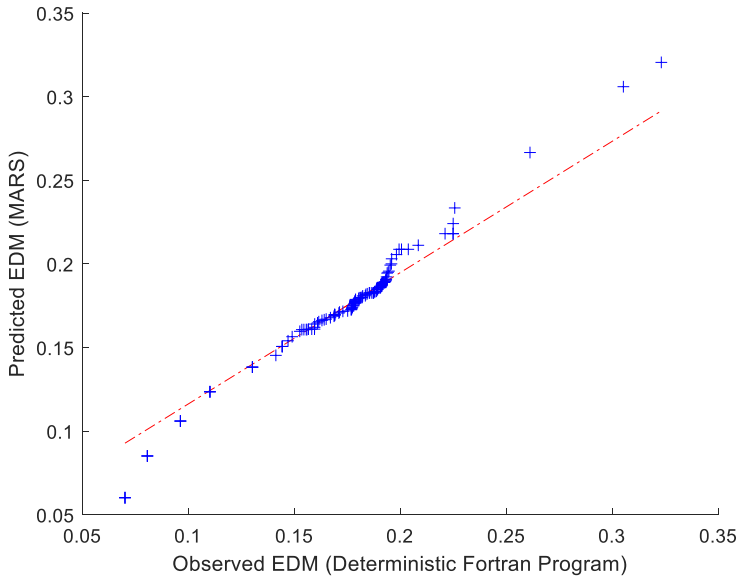

b

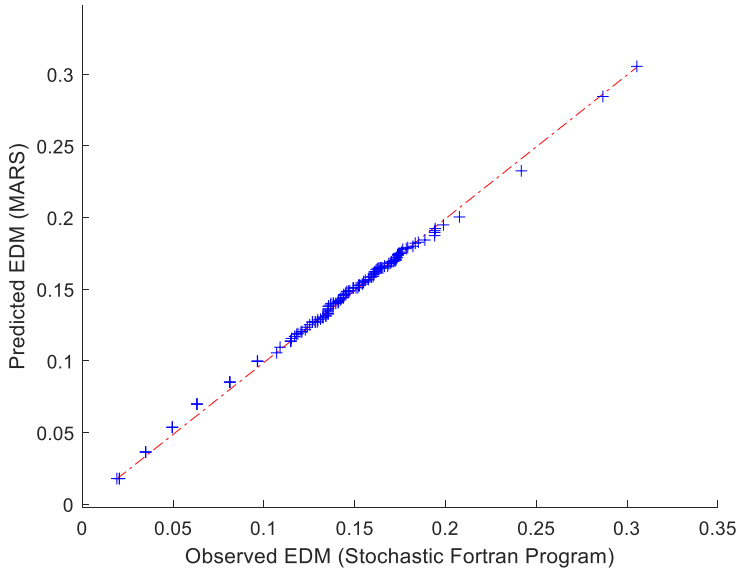

Figure 13. Comparison between MARS model with Fortran program results of the a) deterministic b) probabilistic analysis.

MARS algorithm for achieving to answer uses Backfitting, which is an iterative algorithm and enables MARS to estimate model parameters using all available data, even when some data is missing. In a flexible and efficient manner, it is particularly useful in situations where the relationship between the input variables and the output variable is complex and nonlinear. In order to evaluate the error of the Mars model, the results of modelling by the MARS method to compare the residual sum of squares (RSS) observed in the output of the Fortran code are shown in Figure 14. The values related to the details of the MARS method output along with the GCV error and the penalty value are shown in Figure 15.

a

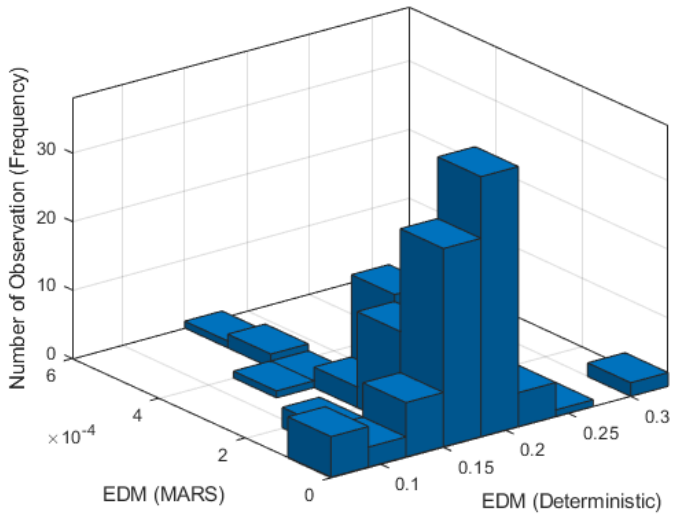

b

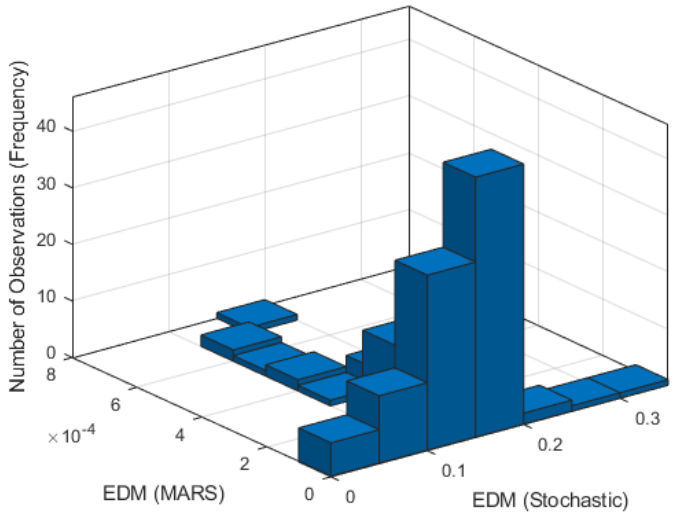

Figure 14. the frequency of the residual sum of squares (RSS) in the MARS model for the a) deterministic b) probabilistic analysis.

a

MARSplines Results:
Dependent: EDM
Independents: Kx/Ky, W/B, Bd/B, H/B, Hu/H, Hd/Hu
Number of terms = 9
Number of basis functions = 8
Order of interactions = 1
Penalty = 2.000000
Threshold = 0.000500
GCV error = 0.000119
Prune = Yes

b

MARSplines Results:
Dependent: EDM
Independents: Kx/Ky, W/B, Bd/B, H/B, Hu/H, Hd/Hu
Number of terms = 10
Number of basis functions = 9
Order of interactions = 1
Penalty = 2.000000
Threshold = 0.000500
GCV error = 0.000127
Prune = Yes

Figure 15. Result of MARS model for the a. deterministic analysis. b. Stochastic analysis

In deterministic analysis, the results indicate that if the ratios of H_u/H_{dam} and H_d/H_u are 0.84 and 0.19, respectively, and K_x/K_y is doubled, the value of EDM will increase by 7.92%. Similarly, if the ratios of H_d/H_u and H_u/H_{dam} are 0.136 and 0.88, respectively, and K_x/K_y is doubled, the value of EDM will increase by 7.6%. Additionally, if the ratio of H_d/H_u is 0.087 and the ratio of H_u/H_{dam} is 0.92, and Kx/Ky is doubled, the EDM will increase by 7.3%. In general, there is a linear relationship between the variables of EDM and K_x/K_y. Assuming a constant geometry of the dam and isotropic earth dam ($K_x=K_y$), with an R^2=0.95, deterministic analysis revealed that a 17.9% increase in the H_d/H_u ratio leads to a significant 29.3% decrease in EDM. This result highlights the importance of accurate estimation of the Hd/Hu ratio in minimizing the EDM.

The probabilistic analysis revealed a different outcome. In the case of an isotropic earth dam ($K_x=K_y$), with a 17.9% increase in the H_d/H_u ratio, the EDM decreased by 19.02%. If assumptions are considered include; H_d/H_u = 0.083, H_u/H_{dam} = 1, H_{dam}/B = 0.25, and W/B = 0.167, then with a 31% increase in Bd/B, the EDM discharge will decrease by 13.12%. The B_d/B and EDM have an inverse relationship with another.

In the case of probabilities, the results of the research show that if the ratios of H_u/H_{dam} and H_d/H_u are 0.19 and 0.84, respectively, and K_x/K_y is doubled, the value of EDM will increase by 23.7%. Similarly, if the ratios of H_d/H_u and H_u/H_{dam} are 0.136 and 0.88, respectively, and K_x/K_y is doubled, the value of EDM will increase by 21.46%. Additionally, if the ratio of H_d/H_u is 0.087 and the ratio of H_u/H_{dam} is 0.92, and Kx/Ky is doubled, the EDM will increase by 19.56%. In general, a linear relationship between the variables of EDM and K_x/K_y is established in a probabilistic analysis.

Comparison of deterministic and probabilistic models

In order to compare deterministic and probabilistic modeling, Table 5 shows the values of errors and fitness. As can be seen, the R-squared (R^2) is 0.93, the Root Mean Square Error (*RMSE*) is 0.012 in the deterministic model, and the values of 0.951 and 0.0138 for the above two values, respectively, in the probabilistic model that show the appropriateness of the model in both. The coefficient of determination for the probabilistic model is better than the deterministic model, but on the contrary, in the *RMSE, MAE, MSE,* and fitness indexes, the values obtained for the deterministic model are more suitable than the probabilistic. In general, according to the above parameters, the deterministic model shows closer proximity to the target model of the FORTRAN code. The deterministic *GCV* error of 1.19×10^{-4} and the stochastic *GCV* error of 1.27×10^{-4} suggest that the deterministic model has a slightly lower prediction error than the stochastic model.

In general, the statistical comparison of this research indicated that MARS could strongly predict the complex relationships between the input and output variables of the seepage problem. In addition, it was able to understand the interaction between input variables during analysis, which is a useful tool for monitoring calculations.

Table 5. Statistical indices for comparing deterministic and probabilistic models.

Parameter	Deterministic	Stochastic
R-square	0.931	0. 951
Adjusted R-square	0.930	0.951
*S_e	0.00929	0.00954
GCV error	0.000119	0.000127
ρ	0.9642	0.9753
RMSE	0.0351	0.0429
RRMSE	0.201	0.301
MAE	0.0097	0.0108
MSE	0.00123	0.00184
RSE	0.0555	0.0758

4. CONCLUSIONS

The study focuses on solving the Laplace equation numerically using the RFEM and incorporating uncertainty components as inputs. The aim is to investigate the impact of uncertainty on estimating seepage flow by employing a hybrid algorithm that combines the RFEM and MARS. In general, the manuscript proceeds in three phases, that in first phase, the FEM was employed under the assumption of deterministic Soil Hydraulic Conductivity (SHC). In the second phase, stochastic analysis was conducted by assuming mean and standard deviation values for SHC. Finally, in the third phase, both deterministic and probabilistic analyses were employed to obtain the EDM with the assistance of the MARS method. In general, it can be concluded about the results of the manuscript that:

i. The study examines the relationship between six dimensionless variables (K_x/K_y, W/B, B_d/B, B_u/B, H_{dam}/B, H_u/H_{dam}, and H_d/H_u) and the EDM. Uncertainty analysis was performed using the MCM, which offers optimal performance and speed compared to other methods, however avoiding high computational costs.

ii. Comparing the models based on statistical parameters (R-square, Adjusted R-square, Se, σ, GCV error, RMSE, RRMSE, MAE, MSE, and RSE) reveals that both models exhibit suitable accuracy, although the deterministic model has a lower percentage of errors.

iii. The comparison of GCV error between the deterministic and probabilistic results using MARS indicates that the deterministic model slightly outperforms the probabilistic model in terms of prediction error for SED. It was found that the deterministic model had a slightly lower estimate error than the stochastic model, with a GCV error of $1.19x10^{-4}$ and $1.27x10^{-4}$, for deterministic and stochastic, respectively.

iv. The evaluation results of the MARS method with the Fortran probability code show that both models have an acceptable performance in predicting dam seepage flow and can be used for future research in the field of Fluid-Structure Interaction (FSI) or Soil-Structure Interaction (SSI) in earth dams.

The list of symbols and notations used in this paper

Symbol	Description	Symbol	Description
H	Height of dam (m)	k	Soil permeability (m/s).
H_d	Downstream water level (m)	φ	Function for SED potential or piezometer head (m).
H_u	Reservoir water level (m)	q	seepage flow rate (m^3/s).
K_x	Horizontal hydraulic conductivity (m/s)	$\{q\}$	SED or inverse SED vector
K_y	Vertical hydraulic conductivity (m/s)	$\{\varphi\}$	Piezometer head vector for nodes.
[T]	Transferred [B] matrix in solid FEM problems	$[K_c]$	The coefficients matrix.
x	The vector of predictor variables.	W_i	The weight function
β0	Intercept term.	N_i	shape function
βj	The coefficients for the basic functions Bj(x).	WS	The weight of the smoothness penalty.
M	The total number of basic functions.	Q	The Normalized SED (m^3/s)
t	Knot point in MARS method	$f_X(x)$	probability mass function or probability density function (PDF),
R^2	Coefficient of Determination	E(g(X))	Monte Carlo estimator
MAE	Mean Absolute Error	fm_i	The sample value obtained from the numerical analysis
RSE	Relative Standard Error	gm_i	Sample value obtained by using MARS
RMSE	Root Mean Square Error	n	Total number of samples
RRMSE	Relative Root Mean Square Error	$\overline{Fm_\iota}$	Average value of the obtained from the numerical analysis in Fortran
EDM	Effective Discharge of MARS method	$\overline{gm_\iota}$	Average value of the sample obtained from MARS.
Q_{mean}	The seepage flow rate from the body of the earth dam(m^3/s).	K_{mean}	The average permeability coefficient body for two vertical axes *Ky* and horizontal *Kx. (m/s)*.
W	Crest width of earth dam.	GCV	a penalty coefficient for validation
B	Bottom width of the earth dam	$G(X_i)$	The LAS algorithm yields the local average value
Bd	The horizontal distance of the dam toe from the downstream side to the crest.	G_i, g_i	Local average of a standard Gaussian random of field over the domain of the *i*th unit
Bu	The horizontal distance of the dam heel from the upstream side to the crest	$G(\tilde{x})$	Correlated function for GRF
k_i	The allocated conductivity of *i*th element	$G_i(\tilde{x})$	Normally distributed random field (with zero mean and unit variance).
geom_freesurf	This subroutine refers to element nodal coordinates and node numbers num for a 2D free surface analysis.	Seep4	This subroutine returns the "analytical" conductivity matrix of a 4-node plane element by using 4 Gauss points.
Coord_g	This subroutine returns to pattern of connecting the nodal points	Num_g	Node Numbering based subroutine in Fortran code
β	The reliability index	k_v	Global conductivity matrix

References

1. Wise, J., Hunt, S. & Al Dushaishi, M. (2023). Prediction of earth dam seepage using a transient thermal finite element model. *Water* 15(7), p. 1423. Doi: 10.3390/w15071423.
2. Kalateh, F., Hosseinejad, F., & Kheiry, M. (2022). Uncertainty Quantification in the analysis of liquefied soil response through Fuzzy Finite Element Method. *Acta Geodynamica et Geomaterialia*, 19(3). Doi: 10.13168/AGG.2022.0007
3. Kalateh, F., & Kheiry Ghoujeh-Biglou, M. (2022). Probabilistic analysis of seepage in earthen dam using Monte Carlo method and with considering permeability of materials and dam geometry. *Irrigation and Drainage Structures Engineering Research*, 23(86), 133-162. Doi:10.22092/idser.2022.358681.1509
4. Kalateh, F., & Kheiry, M. (2022). Finite Elements Modeling of the Seepage through Earth Dam in Isotropic and Non-Isotropic Conditions and Considering the of Downstream and Reservoir Water Level. 2*nd. In International Conference on Architecture, Civil Engineering, Urban Development, Environment and Horizons of Islamic Art in the Second Step Statement of the RevolutionAt.*
5. Zhang, W.G. & Goh, A.T.C. (2013). Multivariate adaptive regression splines for analysis of geotechnical engineering systems. *Computers and Geotechnics* 48, pp. 82–95. Doi: 10.1016/j.compgeo.2012.09.016.
6. Shiau, J., Lai, V.Q. & Keawsawasvong, S. (2023). Multivariate adaptive regression splines analysis for 3D slope stability in anisotropic and heterogenous clay. *Journal of Rock Mechanics and Geotechnical Engineering* 15(4), pp. 1052–1064. Doi: 10.1016/j.jrmge.2022.05.016.
7. Kumar, V., Samui, P., Himanshu, N. and Burman, A. (2019). Reliability-based slope stability analysis of Durgawati earthen dam considering steady and transient state seepage conditions using MARS and RVM. *Indian Geotechnical Journal* 49(6), pp. 650-666.
8. Qureshi, M.U., Mahmood, Z. & Rasool, A.M. (2022). Using multivariate adaptive regression splines to develop relationship between rock quality designation and permeability. *Journal of Rock Mechanics and Geotechnical Engineering* 14(4), pp. 1180–1187. Doi: 10.1016/j.jrmge.2021.06.011.
9. Kumar, R., Metya, S., & Bhattacharya, G. (2022). Probabilistic Evaluation of Liquefaction Potential Using Multivariate Adaptive Regression Splines. Department of Civil Engineering, National Institute of Technology, Jamshedpur.
10. Wang, L., Wu, C., Gu, X., Liu, H., Mei, G. & Zhang, W. (2020). Probabilistic stability analysis of earth dam slope under transient seepage using multivariate adaptive regression splines. *Bulletin of Engineering Geology and the Environment* 79(6), pp. 2763–2775. Doi: 10.1007/s10064-020-01730-0.
11. Zheng, G., Zhang, W., Zhou, H. & Yang, P. (2020). Multivariate adaptive regression splines model for prediction of the liquefaction-induced settlement of shallow foundations. *Soil Dynamics and Earthquake Engineering* 132, p. 106097. Doi: 10.1016/j.soildyn.2020.106097.

12. Vu, D.T., Tran, X.-L., Cao, M.-T., Tran, T.C. & Hoang, N.-D. (2020). Machine learning based soil erosion susceptibility prediction using social spider algorithm optimized multivariate adaptive regression spline. *Measurement* 164, p. 108066. Doi: 10.1016/j.measurement.2020.108066.
13. Deng, Z.-P., Pan, M., Niu, J.-T., Jiang, S.-H. & Qian, W.-W. (2021). Slope reliability analysis in spatially variable soils using sliced inverse regression-based multivariate adaptive regression spline. *Bulletin of Engineering Geology and the Environment* 80(9), pp. 7213–7226. Doi: 10.1007/s10064-021-02353-9.
14. Selçuklu, S., Coit, D., & Felder, F. A. (2022). A Classification of Aleatory and Epistemic Uncertainties in Generation Expansion Planning. Available at SSRN 4216589.
15. Zhang, W., Dai, B., Liu, Z., & Zhou, C. (2017). Unconfined seepage analysis using moving kriging mesh-free method with Monte Carlo integration. *Transport in Porous Media*, 116, 163-180. Doi:10.1007/s11242-016-0769-9.
16. Ahmed, S.A., Revil, A., Bolève, A., Steck, B., Vergniault, C., Courivaud, J. R. & Abbas, M. (2020). Determination of the permeability of seepage flow paths in dams from self-potential measurements. *Engineering Geology*, 268, 105514. Doi: 10.1016/j.enggeo.2020.105514.
17. Fukumoto, Y., Yang, H., Hosoyamada, T. & Ohtsuka, S. (2021). 2-D coupled fluid-particle numerical analysis of seepage failure of saturated granular soils around an embedded sheet pile with no macroscopic assumptions. *Computers and Geotechnics* 136, p. 104234. Doi: 10.1016/j.compgeo.2021.104234.
18. Su, H., Li, J., Wen, Z., Guo, Z., & Zhou, R. (2019). Integrated certainty and uncertainty evaluation approach for seepage control effectiveness of a gravity dam. Applied Mathematical Modelling, 65, 1-22. Doi: 10.1016/j.apm.2018.07.004.
19. Johari, A., & Talebi, A. (2019). Stochastic analysis of rainfall-induced slope instability and steady-state seepage flow using random finite-element method. International Journal of Geomechanics, 19(8), 04019085. Doi: 10.1061/(ASCE)GM.1943-5622.0001455.
20. Johari, A., & Hooshmand Nejad, A. (2018). An Approach to Estimate Wetting Path of Soil–Water Retention Curve from Drying Path. *Iranian Journal of Science and Technology, Transactions of Civil Engineering*, 42(1), 85-89. Doi:10.1007/s40996-017-0074-z.
21. Zhao, X., Shang, S., Yang, Y., & Hu, M. (2021). Three-Dimensional Stochastic Seepage Field Analysis of Multimedia Embankment. *Advances in Civil Engineering*. Doi: 10.1155/2021/1936635.
22. Johari, A., Talebi, A. & Heydari, A. (2020). Prediction of discharge flow rate beneath sheet piles using gene expression programming based on scaled boundary finite element modelling database. *Scientia Iranica* 0(0), pp. 0–0. Doi: 10.24200/sci.2020.53281.3158.
23. Kalateh, F., & Kheiry, M. (2023). Stochastic analysis in the Simulation of Effective Seepage Flow through Earth dams with the Monte Carlo Simulation and Machine Learning. *Water and Soil Management and Modelling*, (), -. Doi: 10.22098/mmws.2023.12184.1208.
24. Smith, L. & Griffiths, D. (2004). Programming the finite element method. John Wiley & Sons.

25. Hassanzadeh, Y., & Abbaszadeh, H. (2023). Investigating Discharge Coefficient of Slide Gate-Sill Combination Using Expert Soft Computing Models. Journal of Hydraulic Structures, 9(1), 63-80.
26. Daneshfaraz, R., Norouzi, R., Abbaszadeh, H., & Azamathulla, H. M. (2022). Theoretical and experimental analysis of applicability of sill with different widths on the gate discharge coefficients. Water Supply, 22(10), 7767-7781.
27. Kalateh, F., Hosseinejad, F., & Kheiry, M. (2022). UNCERTAINTY QUANTIFICATION IN THE ANALYSIS OF LIQUEFIED SOIL RESPONSE THROUGH FUZZY FINITE ELEMENT METHOD. Acta Geodynamica et Geomaterialia, 19(3).
28. Emami, S., Choopan, Y., Kheiry Goje Biglo, M., & Hesam, M. (2020). Optimal and Economic Water Allocation in Irrigation and Drainage Network Using ICA Algorithm (Case Study: Sofi-Chay Network). Irrigation and Water Engineering, 10(3).
29. Abbaszadeh, H., Daneshfaraz, R., & Norouzi, R. (2023). Experimental Investigation of Hydraulic Jump Parameters in Sill Application Mode with Various Synthesis. Journal of Hydraulic Structures, 9(1), 18-42.
30. Ghojeh-biglou, M. K., & Pilpayeh, A. (2019). Effect of geometric specifications of ogee spillway on the volume variation of concrete consumption using genetic algorithm. Revista INGENIERÍA UC, 26(2), 145-153.
31. Abbaszadeh, H., Norouzi, R., Süme, V., Daneshfaraz, R., & Tarinejad, R. (2023). Discharge coefficient of combined rectangular-triangular weirs using soft computing models. Journal of Hydraulic Structures, 9(1), 98-110.
32. Daneshfaraz, R., Norouzi, R., Abbaszadeh, H., Kuriqi, A., & Di Francesco, S. (2022). Influence of sill on the hydraulic regime in sluice gates: an experimental and numerical analysis. Fluids, 7(7), 244.
33. Friedman, J.H. (1991). Multivariate adaptive regression splines. *The Annals of Statistics* 19(1), pp. 1–67. Doi: 10.1214/aos/1176347963.
34. Ju, X., Chen, V.C.P., Rosenberger, J.M. & Liu, F. (2021). Fast knot optimization for multivariate adaptive regression splines using hill climbing methods. *Expert systems with applications* 171, p. 114565. Doi: 10.1016/j.eswa.2021.114565.
35. Hodson, T. O. (2022). Root-mean-square error (RMSE) or mean absolute error (MAE): When to use them or not. Geoscientific Model Development, 15(14), 5481-5487.
36. Daneshfaraz, R., Norouzi, R., Abbaszadeh, H., & Azamathulla, H. M. (2022). Theoretical and experimental analysis of applicability of sill with different widths on the gate discharge coefficients. Water Supply, 22(10), 7767-7781. https://doi.org/10.2166/ws.2022.354
37. Kouhpeyma, A., Kilanehei, F., Hassanlourad, M. & Ziaie-Moayed, R. (2022). Numerical and experimental modelling of seepage in homogeneous earth dam with combined drain. *ISH Journal of Hydraulic Engineering* 28(3), pp. 292–302. Doi: 10.1080/09715010.2021.1891469.
38. Silva, A.V., Neto, S.A.D. and de Sousa Filho, F.D.A. (2016). A Simplified Method for Risk Assessment in Slope Stability Analysis of Earth Dams Using Fuzzy Numbers. *Elecronic Journal of Geotechnical Engineering*, 21(10), 3607–3624. Doi: 10.1016/j.jrmge.2022.05.016

39. Kalateh, F. & Hosseinejad, F. (2020). Uncertainty assessment in hydro-mechanical-coupled analysis of saturated porous medium applying fuzzy finite element method. *Frontiers of Structural and Civil Engineering* 14(2), pp. 387–410. Doi: 10.1007/s11709-019-0601-z.
40. Gui, S., Zhang, R., Turner, J.P. & Xue, X. (2000). Probabilistic Slope Stability Analysis with Stochastic Soil Hydraulic Conductivity. *Journal of Geotechnical and Geoenvironmental Engineering* 126(1), pp. 1–9. Doi: 10.1061/(ASCE)1090-0241(2000)126:1(1).